Theoretical Notes
Note 303

MRC-R-444

EFFECTS OF TERRAIN ON THE EMP
FROM SURFACE BURSTS

John Lavery

Conrad L. Longmire

February 1979

SECURITY CLASSIFICATION OF THIS PAGE (When Data Entered)

REPORT DOCUMENTATION PAGE		READ INSTRUCTIONS BEFORE COMPLETING FORM
1. REPORT NUMBER	2. GOVT ACCESSION NO.	3. RECIPIENT'S CATALOG NUMBER
4. TITLE (and Subtitle) EFFECTS OF TERRAIN ON THE EMP FROM SURFACE BURSTS		5. TYPE OF REPORT & PERIOD COVERED
		6. PERFORMING ORG. REPORT NUMBER MRC-R-444
7. AUTHOR(s) John Lavery Conrad L. Longmire		8. CONTRACT OR GRANT NUMBER(s) F29601-77-C-0020
9. PERFORMING ORGANIZATION NAME AND ADDRESS Mission Research Corporation 735 State Street Santa Barbara, CA 93102		10. PROGRAM ELEMENT PROJECT TASK AREA & WORK UNIT NUMBERS
11. CONTROLLING OFFICE NAME AND ADDRESS Air Force Weapons Laboratory Kirtland Air Force Base New Mexico 87117		12. REPORT DATE February 1979
		13. NUMBER OF PAGES 23
14. MONITORING AGENCY NAME & ADDRESS(if different from Controlling Office)		15. SECURITY CLASS (of this report) Unclassified
		15a. DECLASSIFICATION DOWNGRADING SCHEDULE

16. DISTRIBUTION STATEMENT (of this Report)

17. DISTRIBUTION STATEMENT (of the abstract entered in Block 20, if different from Report)

18. SUPPLEMENTARY NOTES

19. KEY WORDS (Continue on reverse side if necessary and identify by block number)

Electromagnetic Pulse (EMP)
Nuclear Explosions
Effects of Nuclear Explosions

20. ABSTRACT (Continue on reverse side if necessary and identify by block number)

This report discusses the effect of non-flat ground terrain on the EMP from nuclear explosions on the surface. It is shown that some effects cause an increase in the vertical electric field. Calculations to evaluate these effects are recommended.

DD FORM 1473 JAN 73   EDITION OF 1 NOV 65 IS OBSOLETE

SECURITY CLASSIFICATION OF THIS PAGE (When Data Entered)

CONTENTS

1. INTRODUCTION AND SUMMARY ·

This report presents estimates of the effects of non-flat terrain on the EMP produced by nuclear surface bursts. Detailed calculations of the EMP from surface bursts have always been based on the assumption of a perfectly flat earth. Hence one of the present sources of uncertainty in EMP environments arises from non-ideal terrain in practical situations.

The type of terrain envisioned in this study is that found in the bowl-shaped valleys between mountain ranges in Arizona and Nevada. These valleys often have a very flat lake bed at the bottom, surrounded by sloping, rolling terrain crossed by arroyos of various sizes. As typical terrain profiles we shall consider the two sketched in figure 1, that is, either a hill or a valley. The ratio of the height or depth d to the half-width D of the feature will be taken to be generally of the order of 1/5. The magnitude of D will be taken to range from 100 to 1000 meters. Smaller features are not likely to be chosen as sites for military installations, and larger features tend to contain the entire EMP source region. We do not consider the rugged terrain of the mountain ranges.
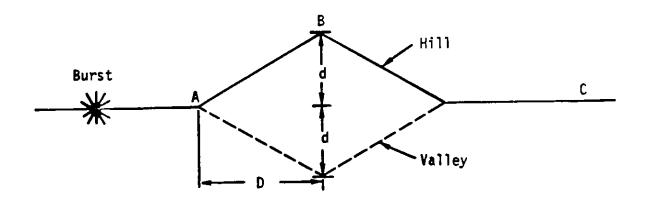

Figure 1. Idealized Terrain Feature

The effect of the terrain, most simply stated, is that some portions, like segment AB in figure 1, receive the direct gammas from the burst but at an angl above tangent; other portions, like segment BC, tend to be shadowed from the direct gammas. These two conditions appear to encompass those to be found in a general terrain.

Our chief interest in this study is to look for conditions under which the EMP is increased by the non-flatness, since we cannot count on the bursts going off in locations that always lead to reductions.

The effects on segment AB are similar to those for a burst above a flat surface, i.e., for a conventional near-surface burst. It is known that the local EMP is not much different from that in the flat-earth surface burst case. The peak fields and later fields are nearly the same. The chief difference is that the high-frequency radiated signal goes off principally in the direction of specular reflection of the ray from the burst point to the local terrain. Since near-surface bursts are considered elsewhere in the AFWL EMP environment program, we shall not discuss this case further in this report.

Thus we have left to consider the effects in the shadowed regions. We divide the problem into two parts. First, we discuss the effects of terrain on the gamma sources and transport, which determine the Compton current and air conductivity. Second, we discuss the effects on the electromagnetic fields produced.

The analysis of transport in Section 2 shows that gamma shadows are deep at early times, when scattered gammas arrive too late. At late times (longer than a few microseconds), scattered gammas can fill in behind relatively gentle terrain features.

Section 3.1 shows that the EMP in the deep shadows at early times, in the attenuated wave phase, is not significantly less than in the flat earth case. Section 3.2 points out a tendency for the vertical electric field in the diffusion phase in shadowed air to be larger than in the

3

flat earth case. Section 3.3 shows that the vertical electric field in the
quasistatic phase can be a few times larger in shadowed regions than in
the flat earth case. The arguments of Sections 3.2 and 3.3 are neither
precise nor thoroughly developed. We recommend further work on these
phases, for example, with the LEMP code.

2. GAMMA SOURCES AND TRANSPORT

In order to estimate the effect of the shadowing, it is necessary
to understand some general properties of the gamma sources and propagation.
The gammas that generate most of the EMP arise from the sources listed in
Table 1.

The extent of shadowing provided by a terrain feature depends on the
effective geometrical size of the gamma source. Note that only the prompt
gammas come from a point source. The ground capture gammas all enter
the air at ground level. The other sources are hemispherical in the air,
and can "see over" smaller terrain features. Even for a point source,
scattering of the gammas by air tends to fill in the shadowed regions.
The scattering problem is analyzed approximately in the following two
subsections.

2.1 Scattering of a Beam of Gammas

We consider a pencil beam of gammas entering a uniform scattering
medium. We wish to calculate how the angular distribution of gamma ve-
locities spreads out around the forward direction and how, as a result,
the radius of the beam grows. We shall look for a steady state solution,
and use the approximation that gamma scattering is confined to fairly
small angles. The Fokker-Planck form of the Boltzmann equation is ap-
propriate for this problem. Let the beam be oriented initially along
the z-axis, let x, y be transverse coordinates, and let v_x and v_y be the
(small) *angles* of deviation of gamma velocity from the z-direction. Then

4

Table 1

PROPERTIES OF GAMMA SOURCE

Gammas	Source	Time Frame	Mean Radius of Source	Average Gamma Energy
Prompts	Bomb itself	$t < 1$ µsec	Point for EMP purposes	1.5 MeV
Air Inelastic	Inelastic scatter of fast neutrons in air	1 µsec $< t <$ 20 µsec	~300 meters, peaked near burst point (hemi-sphere)	4
Ground Captures	Neutron capture in soil	20 µsec $< t <$ 2 millisec	~100 meters, peaked near burst point (circle on ground)	3
Air Captures	Capture of neutrons in air	2 millisec $< t <$ 0.2 sec	~300 meters (hemi-sphere)	6
Fission Fragment Gammas	Fission debris in fireball	$t > 0.2$ sec	Several hundred meters, depending on yield (hemisphere)	1

the Boltzmann equation for the distribution function $f(z,x,y,v_x,v_y)$ is approximately

$$\frac{\partial f}{\partial z} + v_x \frac{\partial f}{\partial x} + v_y \frac{\partial f}{\partial y} = D\left(\frac{\partial^2}{\partial v_x^2} + \frac{\partial^2}{\partial v_y^2}\right)f \tag{1}$$

Here D is a diffusion coefficient related to the single scattering angular distribution, to be evaluated below.

We have found a useful similarity solution of equation (1). Let $\vec{r} = (x,y)$, $\vec{v} = (v_x,v_y)$, and let $R(z)$ and $T(z)$ be functions of z alone. Then

$$f = \frac{1}{\pi^2 R^2 T} \exp\left\{-\frac{r^2}{R^2} - \frac{\left(\vec{v} - \frac{R'}{R}\vec{r}\right)^2}{T}\right\} \tag{2}$$

is a solution of equation (1) provided R and T satisfy

$$R'' = \frac{T}{R} \tag{3}$$

$$T' = 4D - 2\frac{R'}{R}T \tag{4}$$

where the primes indicate differentiation with respect to z. The quantity T is analogous to the transverse temperature of a particle beam and R is a mean radius. Equation (3) is analogous to Newton's law for the expansion, and equation (4) governs the temperature, with collisional heating rate 4D and adiabatic cooling from expansion represented by the second term on the right.

The solution given by equation (2) is normalized to unity for integration over x, y, v_x and v_y.

The relation of D to single scattering can be found by imagining f starts out collimated in angle but uniform in x and y, i.e., an infinite

6

but collimated beam. Then multiply equation (1) by v^2 and integrate over v_x and v_y. We obtain

$$\frac{\partial}{\partial z} \int v^2 f dv_x dv_y = D \int v^2 \left(\frac{\partial^2}{\partial v_x^2} + \frac{\partial}{\partial v_y^2} \right) f \; dv_x dv_y$$

$$= 4D \int f \; dv_x dv_y = 4D \tag{5}$$

Since f starts out collimated, the initial change of the integral on the left must be due to single scattering. Thus

$$D = \frac{1}{4\lambda} \int \theta^2 \; P(\theta) \; 2\pi \sin\theta d\theta \tag{6}$$

where λ is the scattering mean free path and $P(\theta)$ is the normalized angular distribution of scattering. For Compton scattering, a crude estimate of D is

$$D = \frac{1}{2\gamma\lambda} \tag{7}$$

where
$$\gamma = \text{gamma energy}/0.511 \text{ MeV} \tag{8}$$

For the case in which R and T start from zero at z = 0, there is a very simple solution of equations (3) and (4). This solution is

$$T = Dz \approx \frac{1}{2\gamma} \frac{z}{\lambda} \tag{9}$$

$$R = \sqrt{\frac{4D}{3}} \; z^{3/2} \approx \lambda \sqrt{\frac{2}{3\gamma}} \left(\frac{z}{\lambda} \right)^{3/2} \tag{10}$$

7

Equation (10) can also be written as

$$\Theta \equiv \frac{R}{z} \approx \frac{2z}{3\gamma\lambda} \qquad (11)$$

The angle Θ is a measure of how far into a shadow of a ridge (defined by geometrical optics) the scattered gammas reach if they are perfectly collimated when they pass the ridge crest.

If the point source of gammas is located a mean free path or more behind the ridge, the gammas will already have an angular spread when they pass the crest, and so will reach farther into the geometrical shadow than equation (11) indicates. As a beam of initially collimated gammas moves into a scattering medium, the angular spread grows at first (as is indicated by the solution of equations (2), (9) and (10)), but reaches a limit due to energy loss of the gammas in scattering. The energy loss is important for EMP since both the Compton current and the ionization made by a gamma ray are proportional to its energy. We did not include the effect of energy loss in equation (1), which treats the number of gammas rather than their energy content. (The estimate., equation (7), of D was, however, obtained by using the angular distribution of scattered energy rather than photons.) It is possible to treat both scattering and energy loss by means of the Boltzmann equation, but we shall make a very simple estimate of the effect of energy loss.

The energy γ' of a gamma ray scattered at polar angle θ from its original direction is

$$\gamma' = \frac{\gamma}{1 + \gamma(1 - \cos\theta)} \approx \frac{\gamma}{1 + \gamma\theta^2/2}$$

$$\approx \gamma - \gamma^2\theta^2/2 \qquad (12)$$

where γ is the original energy. Thus the energy change is

8

$$\delta\gamma = \gamma' - \gamma \approx -\gamma^2\theta^2/2$$

or

$$\frac{\delta\gamma}{\gamma^2} \approx -\frac{\theta^2}{2} \tag{13}$$

Now let the gamma suffer a sequence of scatterings through polar angles θ_i and azimuthal angles ϕ_i, and let us sum equation (13) over this sequence. Averaging over the azimuthal angles ϕ_i, we have for the total polar angle θ_T (in the small angle approximation)

$$\text{average } \theta_T^2 \approx \sum_i \theta_i^2 \tag{14}$$

Thus the sum of equation (13) leads to

$$\sum \frac{\delta\gamma}{\gamma^2} \approx -\frac{1}{\gamma} + \frac{1}{\gamma_0} \approx -\frac{\theta_T^2}{2} \tag{15}$$

where γ_0 and γ are the energies before and after the sequence of scatterings. Solving for γ, we obtain

$$\frac{\gamma}{\gamma_0} \approx \frac{1}{1 + \gamma_0\,\theta_T^2/2} \tag{16}$$

Thus γ/γ_0 will be reduced by a factor $e \approx 2.7$ at

$$\theta_T \approx \sqrt{\frac{3.4}{\gamma_0}} \tag{17}$$

We compare this result with equation (11) for Θ, obtained without considering energy loss. We see that Θ is less than θ_T for

$$\frac{z}{\gamma} < 5 \text{ mean free paths.} \tag{18}$$

For larger z, θ will be limited by energy loss to the value given by equation (17). If the gamma source is far enough behind the ridge that the angular distribution (17) has already developed, then equation (17) should be used instead of equation (11) to determine the angle of the penumbra in the shadow.

We must remember that the analysis above is based on the assumption of a steady state. Time delays associated with scattered gamma paths make shadow edges more pronounced for the fast-rising prompt gamma pulse, as is discussed in the next subsection. The results of the present sub-section are useful for EMP considerations at retarded times later than a few microseconds.

2.2 Shadows at Early Times

Referring to figure 2, we consider a plane delta function pulse of gammas propagating from left to right, parallel to the z axis. We wish to calculate the gamma flux as a function of time at the point O.
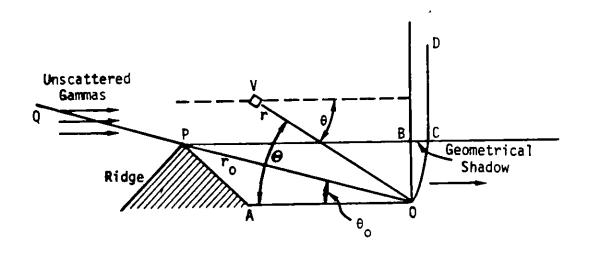

Figure 2. Geometry for Early Time Calculation

The number of unscattered gammas per unit area in the pulse diminishes as $\exp(-z/\lambda)$, where λ is again the scattering mean free path in air. The unscattered gammas have a perfectly sharp and total shadow below the plane PB beginning at the peak P of the ridge. At sufficiently early times, only singly scattered gammas will be significant in the shadowed region.

The very first gammas to arrive at any point in the shadowed region are those scattered in the immediate vicinity of P. When the first gammas arrive at O, the scattered gamma front forms the circle OC about P as center, and the unscattered gamma front is CD. At later times, gammas scattered at other points, such as the volume element V indicated, arrive at O. The time at which these gammas arrive is (c is the speed of light)

$$t_1 = t_B + \frac{r}{c} (1 - \cos\theta)$$

where T_B is the time at which the unscattered gammas arrive at B. The earliest gammas arrive at O at

$$t_0 = t_B + \frac{r_0}{c} (1 - \cos\theta_0)$$

where r_0 is the distance OP. Thus if we choose the time origin at the earliest arrival at O (which is the same as arrival at C), t_1 becomes

$$t_1 = \frac{r}{c} (1 - \cos\theta) - \frac{r_0}{c} (1 - \cos\theta_0) \tag{19}$$

The time dependence of the gammas arriving at O from V is a delta function $\delta(t-t_1)$. To obtain the total time dependence of the gamma flux at O, we have to integrate over the volume above the joined planes QPB.

Let ϕ be the azimuthal angle about the axis OA, measured from the plane of the paper in figure 1. The volume element V thus forms a ring around the axis. The contribution to the scattered flux at O is independent of ϕ, as long as the volume element is above the joined planes

11

QPB. The value ϕ_1 of ϕ at the edge of the contributing volume is given by

for $r < r_0$: $r\sin\theta\cos\phi_1 = r_0\sin\theta_0$, or $\cos\phi_1 = \dfrac{r_0\sin\theta_0}{r\sin\theta}$

$$\left.\begin{array}{l}\\ \\ \\ \\ \\ \end{array}\right\} \quad (20)$$

for $r > r_0$: $r\sin\theta\cos\phi_1 = r\sin\theta_0$, or $\cos\phi_1 = \dfrac{\sin\theta_0}{\sin\theta}$

The angle ϕ_1 goes to zero on the joined planes QPB. Integration on ϕ, in calculating the total flux, yields a factor $2\phi_1$.

Let N be the number of unscattered gammas per unit area that reach CD. The number at V, to which the scattered source is proportional, is exponentially larger, but there is another exponential decay factor for the distance VO. The product of these two factors is just $\exp(-ct_1/\lambda)$; if a gamma has lived a time t_1 longer, it has travelled a distance ct_1 longer.

Finally, we need to include the probability of scattering at angle θ. Let $\sigma(\theta)$ be the differential scattering cross section per unit solid angle at θ and let σ_T be the total cross section. Then define

$$G(\theta) = \sigma(\theta)/\sigma_T \qquad (21)$$

G would equal $1/4\pi$ if the scattering were isotropic.

In terms of the quantities defined above, the total gamma flux at O is

$$F(t) = \frac{N}{\lambda} \int G(\theta) \frac{e^{-ct_1/\lambda}}{r^2} \delta(t-t_1)\, 2\phi_1\, r^2 dr\, d(\cos\theta) \qquad (22)$$

We do the integration on $\cos\theta$ first, using up the delta function. This integration yields a factor c/r, from equation (19), and puts $t_1 = t$ in

the rest of the integrand. The result is

$$F(t) = 2N \frac{c}{\lambda} e^{-ct/\lambda} \int G(\theta)\phi_1 \frac{dr}{r} \qquad (23)$$

In the integrand, θ is determined from equation (19), with t_1 replaced by
t, and ϕ_1 is determined from equation (20). The evaluation of the integrand
is facilitated if the angle θ_0 is small and if we restrict our attention
to small times t, in which case θ is also small and r is near r_0. Then
equation (19) becomes

$$t \approx \frac{r}{2c} \theta^2 - t_0 \qquad (24)$$

with

$$t_0 \equiv \frac{r_0}{2c} \theta_0^{\,2} \qquad (25)$$

Solving for θ, we find

$$\theta = \sqrt{\frac{2c}{r}(t_0+t)} = \sqrt{\frac{2ct_0}{r}\left(1+\frac{t}{t_0}\right)}$$

$$= \theta_0 \sqrt{\frac{r_0}{r}\left(1+\frac{t}{t_0}\right)} \qquad (26)$$

In the small angle approximation, equation (20) becomes

$$\text{for } r < r_0: \quad \phi_1 \approx \sqrt{2\left(1 - \frac{r_0\theta_0}{r\theta}\right)}$$

$$\text{for } r > r_0: \quad \phi_1 \approx \sqrt{2\left(1 - \frac{\theta_0}{\theta}\right)}$$

13

Using equation (26), these become

$$\text{for } r < r_o: \quad \phi_1 = \sqrt{2\left(1 - \sqrt{\frac{r_o}{r}} \Big/ \sqrt{1 + \frac{t}{t_o}}\right)}$$

$$\text{for } r > r_o: \quad \phi_1 = \sqrt{2\left(1 - \sqrt{\frac{r}{r_o}} \Big/ \sqrt{1 + \frac{t}{t_o}}\right)}$$

$$\left.\right\} \quad (27)$$

Note that when $t \ll t_o$, ϕ_1 goes to zero in each case when r is not far from r_o. This implies, by equation (26), that θ is never far from θ_o (scattering comes from near the point P for small t), so that $G(\theta)$ can be replaced by $G(\theta_o)$ and taken outside the integral in equation (23). Then changing the variable of integration to

$$x = \sqrt{\frac{r_o}{r}} \quad \text{for } r < r_o$$

$$x = \sqrt{\frac{r}{r_o}} \quad \text{for } r > r_o$$

$$\left.\right\} \quad (28)$$

we find that the contributions to the integral from $r < r_o$ and from $r > r_o$ are equal, and

$$F(t) = 8N \frac{c}{\lambda} G(\theta_o) e^{-ct/\lambda} \int_1^{\sqrt{1+t/t_o}} \sqrt{2(1 - x/\sqrt{1+t/t_o})} \, \frac{dx}{x} \quad (29)$$

Now, since the radical varies more rapidly than $1/x$, we may replace $1/x$ by unity, and the integral is elementary. The result is

$$F(t) \approx \frac{16\sqrt{2}}{3} N \frac{c}{\lambda} G(\theta_o) e^{-ct/\lambda} \frac{(\sqrt{1+t/t_o} - 1)^{3/2}}{(1+t/t_o)^{3/2}} \quad (30)$$

14

In the approximation $t \ll t_0$, which we have used above anyway, this becomes

$$F(t) \approx \frac{8}{3} N \frac{c}{\lambda} G(\theta_0) \left(\frac{t}{t_0}\right)^{3/2} \tag{31}$$

Here we have dropped the factor $e^{-ct/\lambda}$; by the time (microseconds) this factor is appreciably different from unity, multiple scattering is important.

The result, equation (30), is an upper bound to the single scattering, and is not a bad estimate, even for t as large as $3t_0$.

Integration of F(t), as given by equation (31), from o to t gives

$$\int_0^t F(t)dt \simeq \frac{16}{15} N \frac{ct_0}{\lambda} G(\theta_0) \left(\frac{t}{t_0}\right)^{5/2} \tag{32}$$

For small θ_0, $G(\theta_0)$ is of order of magnitude unity. Using equation (25) for t_0, we find the ratio

$$\frac{1}{N} \int_0^t F(t)dt \simeq \frac{1}{2} \frac{r_0 \theta_0^2}{\lambda} \left(\frac{t}{t_0}\right)^{5/2} \tag{33}$$

Thus at early times the integrated flux is small compared with N (the integrated flux of unscattered gammas).

It is also interesting to fold the delta function response, equation (31), with an unscattered gamma flux rising as $F_0 e^{\alpha t}$. Then the scattered flux is

$$F(t) \approx F_0 e^{\alpha t} \left\{ 2\sqrt{\pi} \frac{c}{\alpha \lambda} \frac{1}{(\alpha t_0)^{3/2}} \right\} \tag{34}$$

15

The quantity in brackets here is usually a small number; $c/\alpha\lambda$ is of the order of 10^{-2} and $\alpha t_0 > 1$ is required for our approximations to be valid. Thus the early time flux in the shadow is very small compared with that in the main beam.

3. EFFECT OF SHADOWS ON EMP

3.1 Effect of Shadows in the Attenuated Wave Phase

We have seen that at early times the gamma shadow created by a ridge in the terrain is quite sharp. This fact suggests that we consider the EMP developed near the plane boundary between exposed and unexposed non-conducting air. This contrasts with the usual problem of determining the EMP that develops at the boundary between exposed air and a conducting ground.

We use Cartesian geometry, with the gammas propagating in the z direction (horizontal), the x-axis vertical, and the y-axis ("azimuthal" about burst point) also horizontal. The fields present are E_z, E_x and B_y. We make our usual transformation to retarded time τ and outgoing and ingoing fields F and G (ref. 1),

$$\tau = ct - z \tag{35}$$

$$F = E_x + B_y \tag{36}$$

$$G = E_x - B_y \tag{37}$$

At early times the ingoing field is negligible, and Maxwell's equations are approximately

$$\frac{\partial F}{\partial z} + 2\pi\sigma F = \frac{\partial E_z}{\partial x} \tag{38}$$

$$\frac{\partial E_z}{\partial z} + 4\pi\sigma E_z = -4\pi J_z + \frac{1}{2}\frac{\partial F}{\partial x} \tag{39}$$

---

1. Longmire, C. L., "Theory of the EMP from Nuclear Surface Bursts," LANC-R-8, January 1970. See also Longmire, C. L., IEEE Trans. on Antennas and Propagation, Vol. AP-26, No. 1, p. 3 (January 1978).

Here J_z is the Compton current and σ is the air conductivity, which both vanish in the shadowed region $x < 0$. In the exposed region $x > 0$, J_z and σ are given by

$$J_z = -J_0 \, e^{\beta\tau - z/\lambda} \tag{40}$$

$$\sigma = \sigma_0 \, e^{\beta\tau - z/\lambda} \tag{41}$$

We have chosen an exponentially rising gamma source proportional to $e^{\alpha t}$, and

$$\beta = \alpha/c \tag{42}$$

The gamma scattering mean free path is again denoted by λ.

The solution of equations (38) and (39) is conveniently considered in two phases. In the first phase, the terms involving σ are negligible in both equations. The fields in this phase increase as $e^{\alpha t}$, and we call it the α-wave phase. The next phase is more important, because the fields are larger in it. In this phase, the term $2\pi\sigma F$ in equation (38) is larger in the exposed air than $\partial F/\partial z$, which is of order F/λ. This phase starts when

$$2\pi\sigma \approx 1/\lambda \approx 3\times10^{-5} \text{ cm}^{-1} \tag{43}$$

However, the term $4\pi\sigma E_z$ in equation (39) is still negligible compared with $\partial E_z/\partial\tau$, which is of order $\beta E_z = \alpha E_z/c$. Thus in this phase

$$2\pi\sigma \ll \frac{\alpha}{c} \approx 3\times10^{-3} \text{ cm}^{-1} \tag{44}$$

The only role of α in this phase is to attenuate the outgoing wave F, and we call it the attenuated wave phase.

17

The equations for the attenuated wave phase are therefore

$$\frac{\partial F}{\partial z} = \frac{\partial E_z}{\partial x} \qquad\qquad (45)$$

in shadow

$$\frac{\partial E_z}{\partial \tau} = \frac{1}{2} \frac{\partial F}{\partial x} \qquad\qquad (46)$$

$$F = \frac{1}{2\pi\sigma} \frac{\partial E_z}{\partial x} \qquad\qquad (47)$$

in exposed air

$$\frac{\partial E_z}{\partial \tau} = -4\pi J_z + \frac{1}{2} \frac{\partial F}{\partial x} \qquad\qquad (48)$$

At the bottom of the shadowed region is the ground, which is a fairly good conductor. For simplicity, we take it to be a perfect conductor, so that $E_z = 0$ at the ground. Now equations (45) and (46) permit the solution

$$\begin{aligned} E_z &= 0 \\ F &= \text{independent of } x \text{ and } z \end{aligned} \qquad \text{in shadow} \qquad (49)$$

We shall see that this solution can be connected approximately to a well-behaved solution in the exposed air.

On substituting equation (47) for F in equation (48), we obtain

$$\frac{\partial E_z}{\partial \tau} = -4\pi J_z + \frac{1}{4\pi\sigma} \frac{\partial^2 E_z}{\partial x^2} \qquad\qquad (50)$$

We have to solve this equation with J_z and σ given by equations (40) and (41). Since equation (50) contains no z-derivatives, z is only a parameter, and the variation of J and σ with z can be included in J_0 and

σ_0 as far as equation (50) is concerned; we do this temporarily. Equation (50) permits a similarity solution of the form

$$E_z(x,\tau) = \frac{4\pi J_0}{\beta} e^{\beta\tau} f(u) \qquad (51)$$

where u is the similarity variable

$$u = x \sqrt{\pi\beta\sigma_0} \; e^{\beta\tau/2} \qquad (52)$$

Substituting this form into equation (50), we obtain an equation for f(u),

$$f + \frac{1}{2} u \frac{df}{du} = 1 + \frac{1}{4} \frac{d^2f}{du^2}$$

which, on multiplying both sides by 2u, can be written as

$$\frac{d}{du} u^2 F = 2u + \frac{1}{2} u \frac{d^2f}{du^2}$$

$$= 2u + \frac{1}{2} \frac{d}{du} u \frac{df}{du} - \frac{1}{2} \frac{df}{du} \qquad (53)$$

Integrate this equation from u = 0 (x = 0) to u, and use the fact that f(0) = 0 in order to match E_z = 0 in the shadowed region. The result is

$$u^2 f = u^2 + \frac{1}{2} u \frac{df}{du} - \frac{1}{2} f$$

or

$$\frac{df}{du} = \left(2u + \frac{1}{u}\right) f - 2u \qquad (54)$$

The solution of the homogeneous equation here is

$$f_1 = u e^{u^2} \qquad (55)$$

19

On letting $f = f_1 f_2$, we obtain for f_2

$$\frac{df_2}{du} = -2u/f_1 = -2e^{-u^2}$$

The solution of this equation is

$$f_2 = 2\int_u^\infty e^{-v^2} dv \tag{56}$$

so that the complete solution for f is

$$f = 2ue^{u^2}\int_u^\infty e^{-v^2} dv \tag{57}$$

We see that $f = o$ at $u = o$, as required. It is easy to show that

$$f \to 1 \text{ as } u \to \infty \tag{58}$$

so that the value of E_z deep in the exposed region is

$$E_z \to \frac{4\pi J_o}{\beta} e^{\beta\tau} \tag{59}$$

Since this limit is independent of x, $F \to o$ here according to equation (47). These results mean that the Compton current is simply charging up the capacitance of space.

At the bottom edge $x = o$ of the exposed region, F can be calculated from equations (47), (51) and (57). The result is

$$F(o) = 2\pi E_s \sqrt{\frac{\sigma_o}{\beta}} e^{\beta\tau/2} \tag{60}$$

where E_s is the saturated field,

$$E_s = -\frac{J}{\sigma} = \frac{J_o}{\sigma_o} \tag{61}$$

Note that E_s is independent of time and space (as long as the gamma source rises exponentially). Since $G \ll F$ in this phase, we have from equations (36) and (37),

$$E_x(o) \approx B_y(o) \approx \frac{1}{2} F(o) \tag{62}$$

According to equation (49), this solution is maintained down through the shadowed region to the ground. Note however that, since σ_0 is carrying the z dependence, F depends slowly on z as $e^{-z/2\lambda}$. This violates the solution (49), but only a little if the depth of the shadowed region is small compared with $2\lambda \approx 500$ meters.

We see that the fields in the shadowed region form a transverse wave. The electric field E_x in this wave terminates on Compton electrons near the bottom of the exposed region, and B_y terminates on the current made by these electrons. At the ground, the fields terminate on charges and currents in the ground. Actually, the front of this pulse is circular, like the arc OC in figure 2. There is some reflection from the ground. The field at the ground in this phase is essentially the same as for a surface burst and a flat earth, in the approximation used (see ref. 1).

3.2 Effect of Shadows in the Diffusion Phase

At the end of the attenuated wave phase,

$$\sigma \approx \beta/4\pi \tag{63}$$

and according to equations (60) and (61),

$$E_x \approx E_s \tag{64}$$

When σ exceeds the value (63), we enter the phase of α-saturation, in which the term $4\pi\sigma E_z$ in equation (39) is larger than $\partial E_z/\partial\tau$ in the exposed air. In this phase, G is no longer negligible, but instead, E_x becomes small compared with B_y. The equations in the exposed air are

21

approximately the diffusion equations of the well-known skin effect. This phase is usually called the diffusion phase. In it the electric field tends to become radial, i.e., $E = E_z$. For the flat earth problem, E_z is shorted out by the ground, and the return conduction current shifts to the ground from the air near the ground, making a large B_y. In our present case, there is an insulator between the exposed air and the ground. In this case, the magnetic field does not increase. Instead, the coupling to the ground is capacitive, and the voltage across the shadowed air tends to approach

$$V \to \int_P^B E_s \, dz \tag{65}$$

where E_s is the saturated field and P and B are the points defined in figure 2. If the depth of shadowed air is small compared with the distance PB, the vertical electric field at 0 has the possibility of being substantially greater than in the flat earth case. However, scattered gammas are building up, and the conductivity in the shadowed region does not remain small for very long. We have not yet made a careful analysis for this phase. We propose to do that and also to make numerical calculations using the LEMP code, if support can be provided.

3.3 Effect of Shadows in the Quasistatic Phase

When the skin depth in the exposed air has become comparable to the distance from the burst, diffusion stops, and we enter the quasistatic phase. In this phase, charge deposited by the Compton current is balanced by the conduction current. In the flat earth case, the electric field and conduction current are very nearly in the θ-direction of spherical coordinates, i.e., they arrive at the ground from the vertical direction. If there were an insulating layer of shadowed air between the exposed air and ground, the conduction current in the exposed air would have to be radial, and there would be a very large voltage across the shadowed air, again given by equation (65).

22

However, there is plenty of time for scattered gammas in this phase, which starts typically at times of tens of microseconds. Equations (11) and (17) show that the scattered gammas fill in rather quickly behind terrain features of the sort envisioned in Section 1. Also, in the later parts of this phase, the air-capture gamma source is hemispherical and can see over most terrain features, probably. We expect that the air conductivity near the ground is a few times lower than in the fully exposed air. Thus the vertical electric field at the ground is expected to be a few times larger than that in the flat earth case, in order to carry the current to the ground. This effect also deserves further investigation.